

DIRECT MEASUREMENTS OF COSMIC RAYS

Roberta Sparvoli

Università di Roma Tor Vergata and INFN

Lecture 1

INTERNATIONAL SCHOOL OF COSMIC-RAY ASTROPHYSICS MAURICE M. SHAPIRO

23rd Course: "Multi-Messenger Astroparticle Physics" — 20 - 28 July 2024

Outline of Lecture 1

In this first lecture, we will talk about:

- The Energy Spectrum of Primary Cosmic Rays
- Main research lines & platforms for direct detection
- Low-Energy Cosmic Rays: effects of the Sun and the Earth
- Cosmic Rays measurements: a toy telescope
- Main balloon experiments (past and present)
- Main satellite and Space Station experiments (past and present)

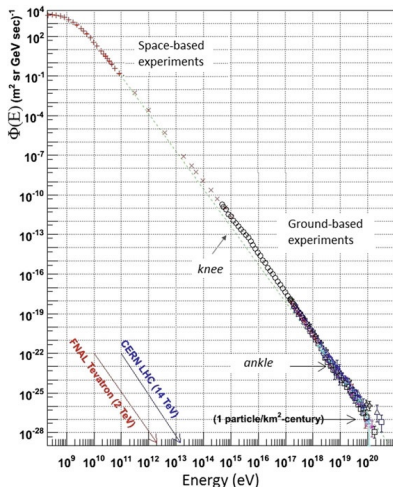
The Energy Spectrum of Primary Cosmic Rays

The solar system is permanently bombarded by a **flux of highly energetic particles, with energies from the MeV range to 10^{20} eV.**

The primary component arriving on the top of the atmosphere includes all **stable charged particles and nuclei**. Also some **unstable nuclei (with lifetimes larger than 10^6 years) are found**.

This (small) fraction of radioactive nuclei is important to estimate the escape time of CRs.

The **energy spectrum of CRs** is shown in the right figure.



The Energy Spectrum of Primary Cosmic Rays

The energy spectrum **falls steeply as a function of energy**. If we consider isotropic the CR flux, we can integrate the integral flux over the solid angle. The integral flux, corresponding to different energy thresholds gives:

$$\mathcal{F}(>10^9 \text{ eV}) \simeq 1,000 \text{ particles/s m}^2$$

$$\mathcal{F}(>10^{15} \text{ eV}) \simeq 1 \text{ particle/year m}^2$$

$$\mathcal{F}(>10^{20} \text{ eV}) \simeq 1 \text{ particle/century km}^2.$$

The energy spectrum of cosmic rays seems almost featureless, but **two transition points are clearly visible**:

- The transition point at $\sim 10^{16}$ eV is called the **knee**. Below the knee, the integral CR flux decreases by a factor ~ 50 when the energy increases by an order of magnitude. Above the knee, the CR flux decreases by a factor ~ 100 when the energy increases by a factor of 10.
- At the energy of 4×10^{18} eV the spectrum becomes flatter again in correspondence of the second transition point, called the **ankle**.

The Energy Spectrum of Primary Cosmic Rays

At energies larger than few GeV **the energy spectrum can be described by a power-law:**

$$\Phi(E) = K \left(\frac{E}{1 \text{ GeV}} \right)^{-\alpha} \frac{\text{particles}}{\text{cm}^2 \text{ s sr GeV}}$$

The parameter α is the differential spectral index of the cosmic ray flux (or the slope of the CR spectrum) and K a normalization factor.

Different compilations of data exist which determine the parameters K , α using direct measurements of the CR flux. These compilations give results in agreement within $\sim 30\%$.

In the energy range from several GeV to 10^{16} eV (the "knee"), cosmic rays follow a power-law with spectral index:

$$\alpha = 2.7$$

$$E < E_{knee} = 10^{16} \text{ eV}$$

The Energy Spectrum of Primary Cosmic Rays

Above the "knee" the spectrum becomes steeper, with an index of approximately:

$$\alpha = 3.0 \qquad E_{knee} < E < E_{ankle}$$

before hardening again above the "ankle" at $\sim E_{ankle} = 4 \times 10^{18}$ eV :

$$\alpha = 2.7 \qquad E_{ankle} < E < E_{GZK}$$

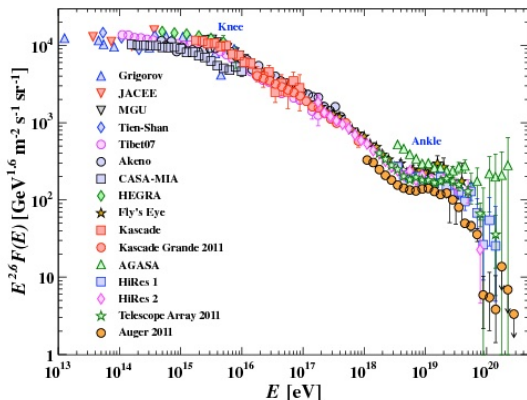
After $E_{GZK} = 4 \times 10^{19}$ eV the spectra measured by ground experiments appear to fall off. This is parametrized by the spectral index:

$$\alpha = 4.2 \qquad E > E_{GZK} = 4 \times 10^{19} \text{ eV}$$

The so-called **Greisen-Zatsepin-Kuzmin (GZK) effect** foresees that **the proton component of the CR flux from sources at cosmological distances drops sharply above the threshold energy E_{GZK} .**

The Energy Spectrum of Primary Cosmic Rays

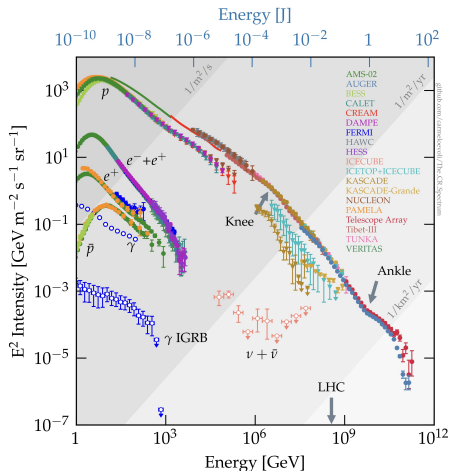
The knee and ankle structures are more evident in this picture. It shows almost the same data set as the other; the difference is that the y-axis variable is multiplied by $E^{2.6}$ to enhance the **visibility for structures in the spectrum**.



Composition of Primary Cosmic Rays

The spectrum presented so far is the so-called "all-particle spectrum". We can disentangle the contribution of the different species:

- about 86% are free protons
- about 11% are alpha particles
- 1% are nuclei of heavier elements up to uranium
- 2% are electrons.
There is also a small percentage of positrons and antiprotons.

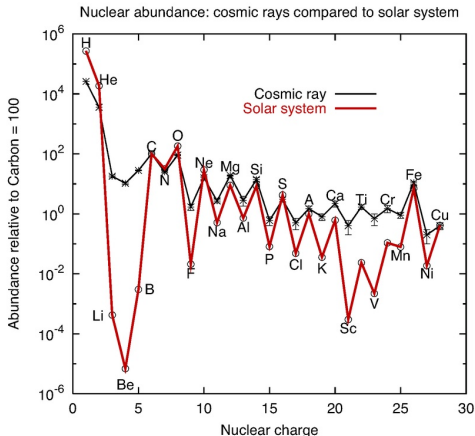


The small flux of electrons does not correspond to a charge-asymmetry in the CR sources. Electrons suffer larger energy losses that reduce the number of those arriving with high energies on Earth.

Composition of Primary Cosmic Rays

We can compare the abundance of the CRs with that of the Solar System. The two samples exhibit a striking similarity:

Both show the odd-even effect, associated with the fact that nuclei with Z and A even are most tightly bound than those with odd A and/or odd Z , so more frequently produced in stars. The normalized peaks in C, N, O, Fe are also similar, suggesting that **the cosmic rays are also produced in stars.**



However, some **remarkable differences between the two exist.**

Composition of Primary Cosmic Rays

The most relevant corresponds to the **overabundance of Li, Be, B elements in CRs with respect to the cosmic chemical composition**. The observed abundance ratio $(\text{Li}+\text{Be}+\text{B})/(\text{C}+\text{N}+\text{O})$ in CRs exceeds the value found in solar system material by a factor of $\sim 10^5$. **A similar excess occurs for the elements below the iron ($Z = 26$) and the lead ($Z = 82$) peaks.**

This difference is interpreted as due to the **effect of the propagation in the Galaxy and provide a measure of the material that CRs have encountered since they were accelerated**.

Carbon, nitrogen, and oxygen are considered primary cosmic rays, produced and accelerated by astrophysical sources. Lithium, beryllium, and boron are secondary components **produced by fragmentation** reactions of the heavier C, N and O elements during the journey of CRs in the interstellar medium.

Direct measurement of Cosmic Rays

Considering the full spectrum of Cosmic Rays, the detection is divided in:

- $E < 100$ TeV: **direct detection**, by space- and balloon-borne experiments above Earth's atmosphere, in which the primary particles are mostly absorbed.

This detection mainly concerns Galactic Cosmic Rays!

CR fluxes measured on Earth are **influenced by their travel through the galactic interstellar medium and magnetic field**. At energies above 30 GeV, where all local effects coming from the Sun or the Earth are not important, **the radiation appears to be isotropic, since the galactic magnetic fields would destroy any initial anisotropy**. → No astronomy with GCRs!

- $E > 100$ TeV: **indirect detection** by ground-based experiments, which measure air showers of secondary particles produced by the primary cosmic-ray particles interacting in Earth's atmosphere.

This detection mainly concerns Cosmic Rays in transition from the Galaxy out! Not necessarily isotropic → Sources?

Main research lines for direct detection

By studying Galactic Cosmic Rays by direct detection, we pursue the following science objectives:

- CR flux reconstruction **up to the highest energy band** (looking for sources and acceleration mechanisms, ...)
- CR **compositions studies** (looking for source material, dust/gas distribution, nucleosynthesis, selection effects, ...)
- CR flux **modulation in the low energy band** (looking for effects from heliosphere/magnetosphere, ...)
- **Antimatter component** in CRs (looking for dark-matter and anti-matter limits, nearby sources, ...)

It is not possible to study all with the same experiment!

According to the physics line, different detections techniques are adopted

Existing platforms

- **Balloon experiments** (CREAM, ATIC, BESS-Polar, TRACER, TIGER&SuperTIGER, ...): very popular in the 80's, but later on they were substituted by satellite. They returned popular especially with the NASA Long and Ultra-long Duration Balloon Program (LDB and ULBD).
- **Satellite experiments** (PAMELA, FERMI, DAMPE, NUCLEON, ...): started from 2000. No residual atmosphere but challenging and expensive. Several constraints imposed on experiments.
- **Space station experiments** (AMS, CALET, ISS-Cream,..)



Low-Energy Cosmic Rays from the Sun

The Sun affects the CRs flux in two ways:

- ◇ **The Sun is the main source of CRs of energy below ~ 4 GeV.** Cosmic rays originated from the Sun consist of protons, electrons and heavy ions with energy from a few tens of keV to few GeV. They are originated mainly by **solar flares**.

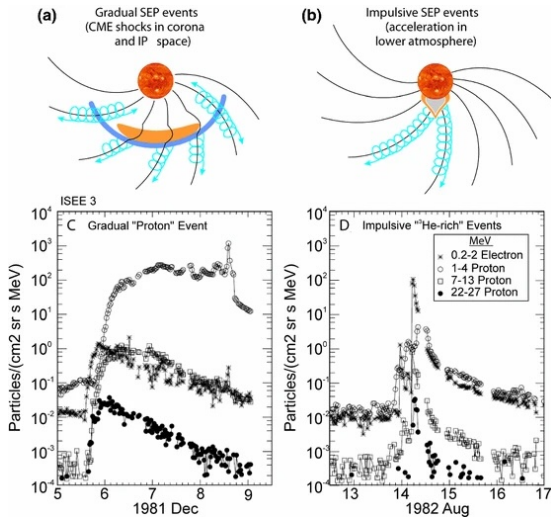
A **solar flare** is a sudden brightening observed over the Sun's surface, interpreted as a large energy release. Flares occur in active regions around **sunspots**, where intense magnetic fields penetrate the photosphere to link the corona to the solar interior.

- ◇ The Sun activity influences also the **probability that CRs with energy below few GeV reach the Earth.** **When CRs enter our solar system, they must overcome the outward-flowing solar wind.**

This wind is a stream of charged particles continuously released from the upper atmosphere of the Sun and it consists mostly of electrons and protons with energies usually between 1.5 and 10 keV.

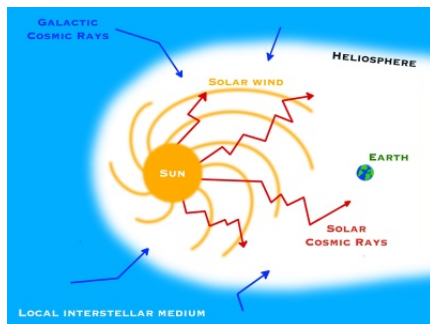
Low-Energy Cosmic Rays from the Sun

In a **Solar Energy Particle (SEP)** events, fluxes increase by orders of magnitude wrt the flux of Galactic Cosmic rays.



Solar modulation

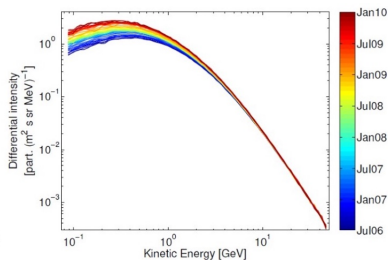
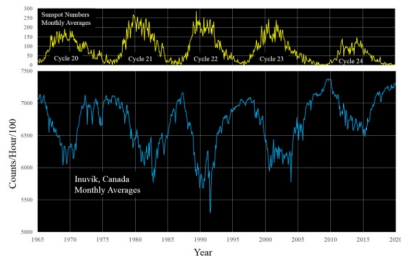
The flux of galactic CR nuclei with energies below ~ 1 GeV/nucleon is strongly modulated by their interaction with the magnetic field carried by the expanding solar wind. **The expanding magnetized plasma generated by the Sun decelerates and partially excludes the lower energy particles from the inner solar system.** Consequently the low-energy component of the CR flux undergoes a sizable variation over the solar cycle. This effect is known as **solar modulation**.



Solar modulation

The magnetic activity and the solar modulations are manifested through sunspots, which have a 11 year cycle. **The intensity of low-energy CRs at Earth is measured through ground-based detectors called neutron monitors**, designed to measure neutrons produced by the interactions of CRs with the atmospheric nuclei. Solar modulation is also clearly visible by space detectors.

CR's measurements are anti-correlated with the level of solar activity, i.e., when solar activity is high many sunspots are visible, the CR intensity at Earth is low, and vice versa.



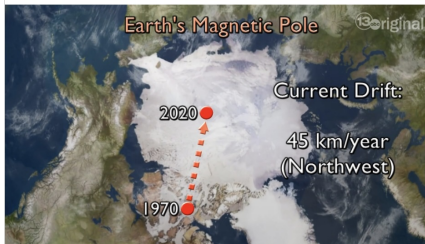
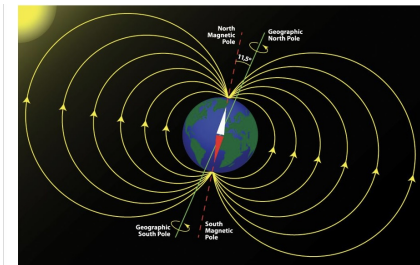
The Earth magnetic field

Originated by electric currents running inside the Earth core.

To a first approximation **it is a dipolar field:**

Coordinates: 79° N; 70° W and 79° S; 110° E, reversed with respect to geographic Poles, about 11° inclined with Earth axis and shifted by 320 km.

The field changes slowly over the years, producing a **secular drift of the magnetic Poles.**

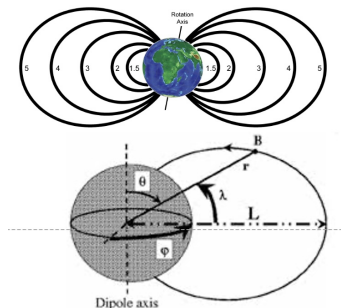


Magnetic field equations: dipole field

The "dipole representation" is accurate to $\sim 30\%$ at distances $\sim 2-3 R_E$.

A better empirical representation is based on a **multipole expansion (International Geomagnetic Reference Field IGRF model)**, with slowly time-dependent coefficients.

To describe the field, also in not-dipole approximation, usually the **Mcllwain coordinates (B,L)** are used.



A point P in space is defined by:

L \rightarrow distance (in R_E) of the field line passing far P, measured on the equatorial plane. A measure of "equatorial radius".

B \rightarrow magnetic field intensity in P. A measure of "latitude".

CRs trajectories in the Earth Magnetic field

Consider a particle of charge Ze with **orbit in the equatorial plane of the dipole-like Earth magnetic field**. Equating the centrifugal and the Lorentz force gives

$$\frac{mv^2}{r} = Ze |\mathbf{v} \times \mathbf{B}|$$

The Earth magnetic field is induced by the Earth magnetic moment M :

$$B = \frac{\mu_0}{4\pi} \frac{M}{r^3}$$

At the surface ($r = R_E = 6.38 \times 10^6 \text{ m}$) the measured value is $B = 0.307 \times 10^4 \text{ T}$, therefore $M = 7.94 \times 10^{22} \text{ Am}^2$. It is easy to work out the radius of the orbit from the 2 previous equations:

$$r = \left(\frac{\mu_0}{4\pi} \frac{ZeM}{p} \right)^{1/2}$$

where p is the particle momentum.

CRs trajectories in the Earth Magnetic field

Using the numerical values for the Earth's radius:

$$\frac{p}{Ze} = \frac{\mu_0}{4\pi} \frac{M}{R_E^2} \sim 59.6 \text{ GV}$$

where GV stands for Gigavolt and it is a measure of the **particle's rigidity**.

This value corresponds to the **minimum rigidity for a particle to be able to reach the Earth**, if its orbit is exactly in the (magnetic) equatorial plane. This value is called **equatorial cut-off rigidity**.

Toward the poles, the influence of the dipole field becomes weaker (as the arriving particle velocity is almost parallel to B), and **the cutoff rigidity becomes smaller**. Thus the integrated CR intensity **increases with the latitude for charged particles (latitude effect)**.

CRs trajectories in the Earth Magnetic field

Let us consider a particle with Z and \mathbf{p} detected at a point \mathbf{x} ; we can **trace back the particle path to its origin** (en electric charge moving in a static non-homogeneous magnetic field). We can find:

- a) the trajectory originates from Earth's surface or in atmosphere;
- b) the trajectory remains confined in the volume $R_E < r < \infty$;
- c) the trajectory reaches infinity.

Trajectories a) and b) are **"forbidden"** because no cosmic rays from far away can reach the Earth along them.

The others are **"allowed"**. Positive particles with rigidity higher than the cut-off are allowed.

The effect of the geomagnetic field is to remove particles from the forbidden trajectories, without deforming their spectrum.

Van Allen Belts: discovery

No attention was given to the "forbidden" orbits, though mathematically known, **until they were truly discovered (Van Allen, Explorer I and II, 1958).**

The Geiger counters onboard above 2000 km seemed to stop working → saturation!

The existence of two radiation belts around the Earth was discovered;

the internal (Inner Belt) full of protons, the external (Outer Belt) rich of electrons.



Van Allen Belts: origin and death

Origin: high energy CR interactions in atmosphere, producing neutrons and then protons and electrons (**CRAND mechanism**).

Also Solar Wind and influences the ionosphere.

Inner Radiation Belt:

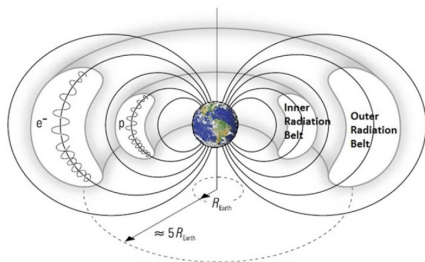
protons with E up to hundreds of MeV.

Mean life time: years.

Outer Radiation Belt:

electrons with E of a few MeV.

Mean life time: days.



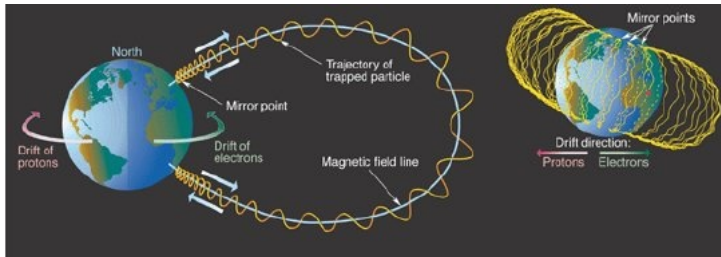
Death: distortions in the magnetic field (also due to solar activity) bring particles to jump to different field lines which go down to dense atmosphere: collisions;

Also collisions among themselves.

Van Allen Belts: particles motion

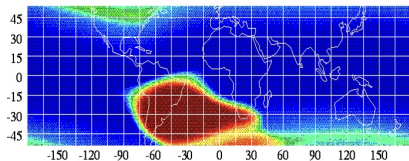
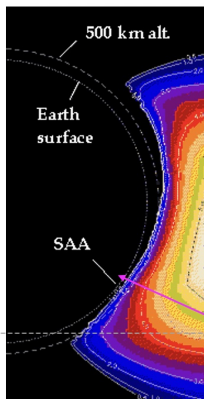
Combination of 3 periodic motions:

- ◇ **Gyration:** a helix around the field line;
- ◇ **Bounce:** oscillation around the equatorial plane between almost symmetrical mirror points. Only small oscillations are possible, the mirror point cannot hit the Earth surface.
- ◇ **Drift:** longitudinal. It is due to dishomogeneity of the field and variations of the gyroradius. Positive particles drift westward, negative eastward.



South Atlantic Anomaly SAA

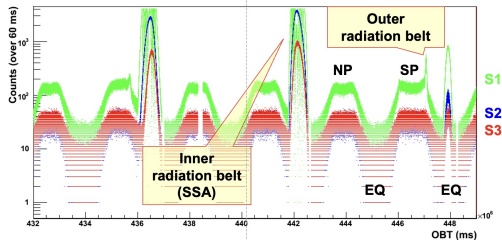
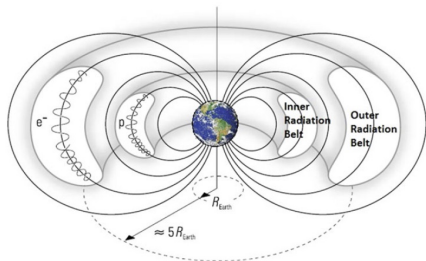
Above South America, about 200 - 300 kilometers off the coast of Brazil, and extending over much of South America, the nearby portion of the Van Allen Belt forms what is called the **South Atlantic Anomaly**.



This is an area of **enhanced radiation** caused by the offset and tilt of the geomagnetic axis with respect to the Earth's rotation axis, which brings part of the radiation belt to **lower altitudes**.

The inner edge of the proton belt dips below the line drawn at 500 km altitude.

Van Allen Belts



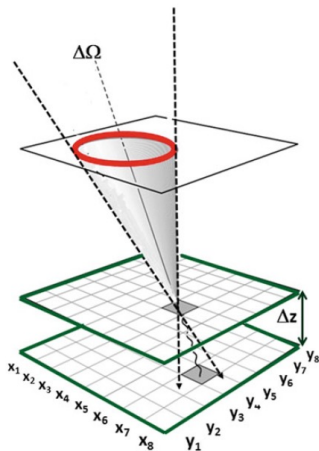
The belts, and especially the South Atlantic Anomaly, pose a **hazard to satellites**, which must protect their sensitive components with adequate shielding if their orbit spends a significant time inside the radiation belts.

Along a satellite polar orbit, the count rate across the SAA saturates.

CR measurements: a toy telescope

Any experimental apparatus for CRs detection should: (i) identify the particle, (ii) measure its electric charge, and (iii) measure its energy and momentum.

Layout of a simple telescope for the measurement of CRs. The two counter's layers are assumed to be segmented both in the x and y axis. A CR arriving within the *solid angle* $\Delta\Omega$ will produce one hit on each *layer*.

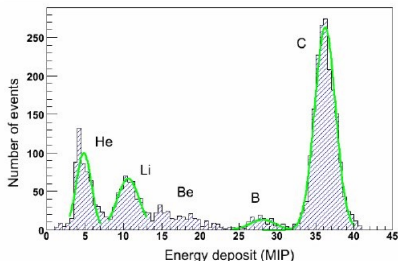


Charge identification: dE/dx measurement

The signal in the counter is provided by the excitation/ionization energy loss of through-going charged particles.

The excitation/ionization energy loss is **proportional to the square of the electric charge Z of the particle**. With **proportional counters** the amplitude I_{hit} of the signal depends thus on Z^2 .

This method to measure the electric charge of the incoming particle through the Bethe-Bloch formula is referred as **dE/dx measurement**.



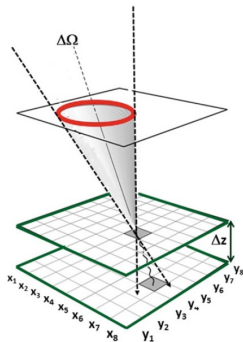
Some experiments have **redundant detectors for the measurement of the electric charge**. This redundancy makes the nuclei selection very clean.

The "hit" recording

In the toy telescope we assume that a charged particle crossing the lower counter induces a signal at the position labeled (x_7, y_4) .

Additional information are the z-position z_1 of the layer, the crossing time (t_1) and the amplitude I_1 of the signal. The complete set of information (**a hit**) can be represented as $(x_7, y_4; z_1, t_1, I_1)$. The hits are stored as digital information on a online computer.

Layout of a simple telescope for the measurement of CRs. The two counter's layers are assumed to be segmented both in the x and y axis. A CR arriving within the *solid angle* $\Delta\Omega$ will produce one hit on each layer



Trigger logic

A major requirement of any experiment is the **trigger logic**. This is a **mandatory task**, because the probability of a **fake signal on a single counter is high**. Due to the presence (for instance) of radioactive elements in the surrounding materials, or due to electronic noise, there are spurious signals in each detector plane with usually larger rates. By definition, these spurious hits are not correlated with a crossing particle and constitute the **background**.

In our simple example, a trigger is given by a **coincidence between planes**. This corresponds to have a signal both on the z_1 and z_2 layers within a given time interval T . A **condition on amplitudes** I_1, I_2 can also be added. **The hits are permanently stored in the computer for further analysis if $|t_1 - t_2| \leq T$** . The combination of signals in both planes, without constraints on time difference, will usually provide a **too large event rate with respect to the real CR rate**.

Time-of-Flight ToF

Relativistic particles in vacuum cover 1 m in ~ 3.3 ns. Typical distances Δz between layers in CR telescopes (as in our example) are of the order of 1-2 m.

The **timing resolution of the detectors** must be of the order of a **ns (or better)** to have the possibility to **distinguish between upward- (with $t_2 - t_1 > 0$) and downward- (with $t_2 - t_1 < 0$) going cosmic rays**. In this case, a **time-of-flight (ToF) measurement is performed**.

A very good timing resolution is characteristic for instance of most **scintillation counters**. Scintillation counters can be arranged in order to have sufficient spatial resolution to distinguish different directions (as in our telescope).

In addition, their response depends on the ionization energy loss, and thus on the particle Z^2 . **Many ToF systems are also used to measure the Z of the detected particle.**

Momentum measurement: magnetic spectrometers

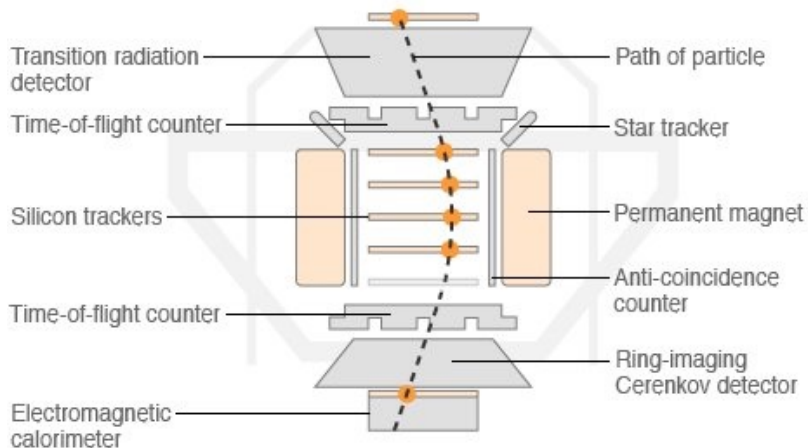
In many detectors a **uniform magnetic field in the region between the counters performing a ToF is present**. The field is generated by a solenoid (either permanent or superconductive).

The magnetic field allows the measurement of the **particle momentum** (if $|Ze|$ is known), as charged particles are deflected **according to their rigidity** (rigidity: $\text{momentum}/|Ze|$), and the **sign of the charge**.

To measure the curved particle trajectory, **additional detectors are needed inside the magnetic field region**. If the magnetic field is along the y axis, $\mathbf{B} = B_y$, the deflection is expected along the x-axis for particles entering with velocity along z. In this case, detectors with **good spatial resolution inside the magnetic field (tracking systems)** are used to accurately measure the x coordinate.

The combination of the magnetic field and tracking detectors forms a **magnetic spectrometer**. It can measure the particle rigidity up to a maximum value that depends on the magnetic field and on the precision of the measurement of the curvature. The **maximum detectable rigidity MDR** is reached when the curvatures are poorly described by arcs, and appear to be straight lines.

Momentum measurement: magnetic spectrometers



Source: CERN

Energy measurement: Cherenkov detectors

In the energy range from the GeV to about 1 TeV, the energy can be measured using magnetic spectrometers (provided one knows charge and mass of the particle) or **Cherenkov detectors**.

Cherenkov radiation occurs when **a particle in a medium moves faster than light in the same medium**. **The coherent wavefront has a conical shape and is emitted at an angle:**

$$\cos \theta = 1/\beta n$$

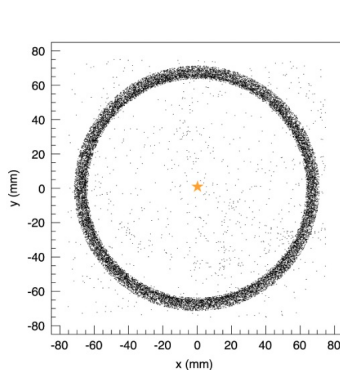
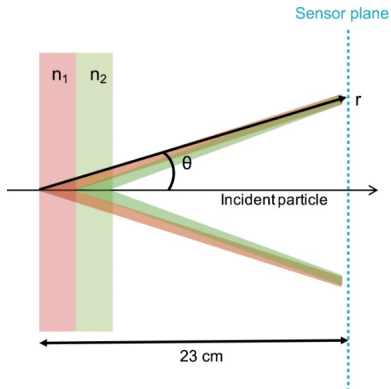
with respect to the trajectory of the particle.

The dependence of the cone emission angle on the particle velocity is used to construct Cherenkov detectors. These detectors provide the best velocity measurements available.

The energy lost due to the Cherenkov effect is **relevant only to relativistic energies**. Even at these speeds, however, the energy loss is relatively low.

Energy measurement: Cherenkov detectors

The **Ring-imaging Cherenkov detector (RICH)** estimates the particle velocity $\beta = v/c$ with a high accuracy. The β derives from **pattern recognition of photons distributed over geometrical shapes** as circles, ellipses, arcs produced by the Cherenkov effect. Charge measurement derives from the **total amount of collected photons**. Higher is the charge, higher is the number of photons.



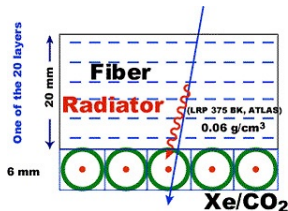
Energy measurement: Transition Radiation Detectors TRDs

At high energy, also **Transition Radiation Detectors (TRDs)** can be used for energy measurements.

TRDs have been used to measure the Γ Lorentz factor of the incident particle and thus the energy. The information from a TRD allows, together with data from other detectors, a separation of different nuclei.

Radiation (in the **X-ray band**, called **transition radiation**) is produced when a particle with high Γ crosses several interfaces characterized by a **change of the refraction index**. Particles with large Γ induce X-rays. For a given energy, **this allows a discrimination between light and heavy particle, as $\Gamma = E/mc^2$.**

A TRD contains many layers of transparent materials with **different indices of refraction n** in order to increase the photon emission probability of a single layer.



Energy measurement: calorimeters

The **calorimetric technique** is another method used for the energy determination of CRs.

In calorimeters, the particles need to be (at least partly) absorbed; the kinetic energy of the incident particle is **converted into a cascade of many secondary particles (the shower)**. At the end, the primary energy of the incident particle is dissipated via excitation/ionization of the absorbing material.

A primary CR interacting with a nucleus produces secondary **hadrons**. They deposit energy through ionization/excitation of the medium and through successive interactions with nuclei, yielding lower energy hadrons, the **hadronic cascade**. Neutral mesons produced in the cascade, mainly π_0 , decay into $\gamma\gamma$ pairs. Each high-energy photon **converts into an electron-positron pairs**; each e^- (e^+) is able to radiate energetic photons through **bremsstrahlung**. These radiated photons can convert into pairs that, in turn, radiate. In conclusion, one has an **electromagnetic shower** with a large number of photons, electrons, and positrons.

Balloon Experiments

The hypothesis of the existence of an extraterrestrial radiation was confirmed with experiments using balloon ascensions. **Balloon experiments were always important during the CR history.**

Scientific balloons used today (for instance for the NASA flights) are made of 20 μm thick polyethylene film; they are as large as a football stadium with a diameter of about 140 m and a volume larger than 1.1 million cubic meters filled with helium gas. **They can carry experiments (payloads) up to 3600 kg and fly at altitudes up to 42 km.** The payloads are attached to a parachute. The flights are terminated by remotely firing an explosive squib that separates the payload from the balloon. **The experiment descends slowly, suspended by the parachute, and it is recovered and refurbished for future flights.**

Apart from the measurement of the **cosmic ray composition in the region below the knee**, balloon experiments as well as detectors on satellites are devoted to searches for **antimatter and dark matter in our Galaxy.**

ATIC (2000) and TRACER Balloon Experiment (2003-2006)

The **Advanced Thin Ionization Calorimeter (ATIC)** was configured with a BGO calorimeter with about $20 X_0$, preceded by a silicon matrix for the measurement of the particle Z .

Since December 2000, ATIC had 3 successful flights from McMurdo, Antarctica. Concerning the measurement of primary CRs composition, the ATIC data filled the gap for elements from protons ($Z = 1$) to iron ($Z = 26$) of the measurements made by experiments using spectrometers and higher energy data from emulsion-based experiments.

The **Transition Radiation Array for Cosmic Energetic Radiation (TRACER)** was configured with two layers of plastic scintillators ($2 \times 2 \text{ m}^2$) and a TRD to determine the Γ of the incident particle. A Cherenkov counter at the bottom of the detector was used to reject non-relativistic particles.

TRACER reported elemental spectra from oxygen ($Z = 8$) to iron ($Z = 26$) from a flight in Antarctica in 2003, and from boron ($Z = 5$) to iron in a second flight in 2006.

CREAM Balloon Experiment (2005-2010)

The **Cosmic Ray Energetics and Mass Balloon Experiment (CREAM)** used both a calorimeter (with 20 radiation lengths X_0 and half interaction length λ_I) and a TRD for the measurements of the CRs energy. The two subdetectors had different systematic biases in determining the particle energy allowing an in-flight cross-calibration of the two techniques for particles with $Z \geq 4$.

The CREAM calorimeter measured all elements, including nuclei with $Z = 1$ and 2, up to about 10^{14} eV with energy resolution better than 45% for all energies. The highly segmented detectors comprising the instrument had about 10^4 electronic channels. The CREAM calorimeter was designed to be large enough to collect adequate statistics, within the weight limit for a balloon flight. It used a tungsten absorber (tungsten has high Z and a small radiation length) and thin scintillating fibers.

From 2005 to 2010, the CREAM payload flew six times, for a cumulative exposure of 162 days and with a record duration of almost 40 days, while circumnavigating Antarctica three times.

CREAM Balloon Experiment (2005-2010)



a CREAM ballooncraft with the launch vehicle while a 10^6 m^3 balloon is being inflated at the launch site, Williams field near McMurdo, Antarctica; **b** the balloon trajectory of a 37 day flight of CREAM, which was launched on December 1, 2009 and terminated on January 8, 2010 during about three rounds of the South Pole.

Comparison of balloon experiments for CR composition

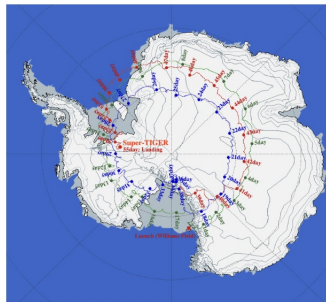
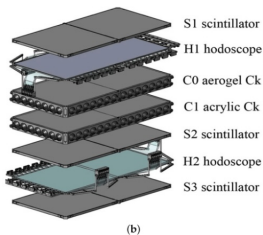
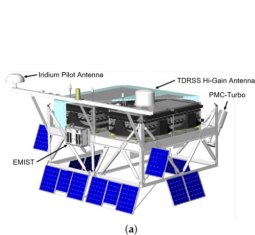
Comparison of balloon experiments for high-energy CR measurements

Instrument	Energy measurement	Charge range	Flight duration (days)	Atmospheric overburden (g/cm^2)	Exposure ($\text{m}^2 \text{ sr days}$)	$N_p E > 6 \text{ TeV}$
ATIC	Calorimeter	$1 \leq Z \leq 28$	48	4.3	5	~ 720
TRACER	TRD	$8 \leq Z \leq 28$	10	3.9	50	–
CREAM	Calorimeter	$1 \leq Z \leq 28$	160	3.9	48	$\sim 5,000$
CREAM	TRD	$3 \leq Z \leq 28$	42	3.9	55	–
JACEE	Emulsion	$1 \leq Z \leq 28$	60	5.3	10	~ 700
RUNJOB	Emulsion	$1 \leq Z \leq 28$	60	10	24	~ 700

The energy measurement techniques are identified in Column 2; the range of the electric charge measurement in Column 3. The charge resolution was $\sim \Delta Z = 0.3$ for all experiments, apart JACEE and RUNJOBS

SUPER-TIGER Balloon Experiment (2012-2019)

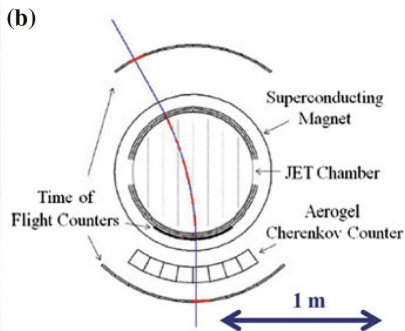
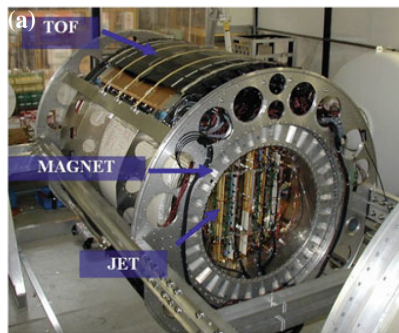
Building on the success of TIGER (launched in 2001 and 2003), SuperTIGER (Super Trans-Iron Galactic Element Recorder) had a record-breaking 55-day flight over Antarctica in December 2012 – January 2013 and a 32-day flight in December 2019 – January 2020.



@Nicole Osborn's talk, this school

BESS Balloon Experiment (2004 - 2007)

In BESS, the rigidity is measured in the superconducting spectrometer, where a uniform B of about 10^4 G acts for 1 m on the particles. The sagitta is measured by drift chambers. The ToF system provides the measurement of the particle direction, velocity $\beta = v/c$ and Ze .



a A picture of the original BESS apparatus. **b** A cross-sectional view of the BESS-Polar instrument showing also a particle trajectory.

BESS Balloon Experiment (2004 - 2007)

BESS has had nine successful flight campaigns since 1993, and additional two over the Antarctica, called BESS-polar.

BESS-Polar I & II flights were carried out over Antarctica.



BESS-Polar I (green),
BESS-Polar II (1st:blue, 2nd:red)

	BESS-Polar I	BESS-Polar II
Launch date	Dec. 13 th , 2004	Dec. 23 rd , 2007
Observation time	8.5 days	24.5 days
Cosmic-ray observed	9×10^8 events	4.7×10^9 events
Flight altitude	37~39km (5~4g/cm ²)	~36km (6~5g/cm ²)

Satellite and Space Station experiments

Starting from the 90's, when the technology was ready, balloon experiments started to be substituted by experiments carried out on **satellites** or on orbiting **Space Stations**.

With respect to balloons, satellite experiments have advantages and disadvantages. Among them we can mention:

Adv. : much longer data-taking → years instead of days/weeks;

Adv. : complete absence of residual atmosphere → no necessity to correct the fluxes for the interaction in the upper layers of the atmosphere;

Disadv. : no possibility to recover the payload after the mission;

Disadv. : higher costs and risks.

Satellite and Space Station experiment **are analogous but** on ISS:

- ◇ Bigger detector mass&dimensions ☺;
- ◇ Fewer launchers and docking possibilities ☺;
- ◇ Higher geomagnetic cut-off (almost equatorial orbit) ☺!

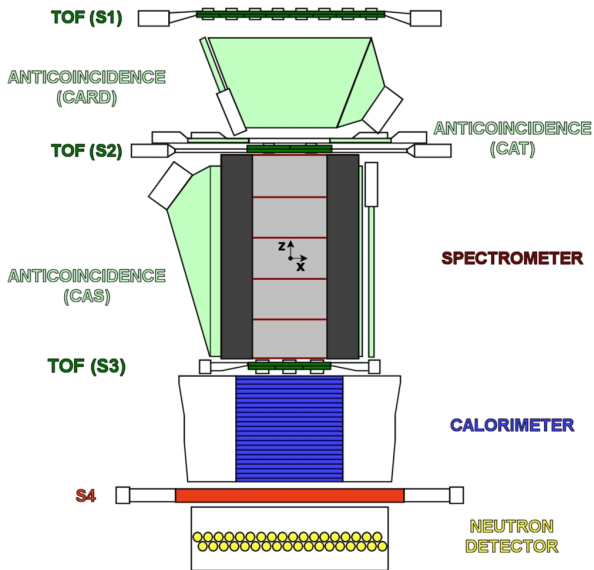
The PAMELA experiment (2006-2016)

The **Payload for Antimatter Matter Exploration and Light-nuclei Astrophysics (PAMELA)** was an experiment mainly devoted to antimatter studies up to the hundreds GeV region. Its size and flight duration were such as to allow an accurate measurement of the neutral and charged components of CRs up to the TeV region. PAMELA satellite was launched by a **Soyuz-U rocket in June 2006**, on board a Russian satellite of the class **Resurs-DK1** on a polar orbit. Its life ended in **January 2016, after almost 10 years of data-taking.**

The apparatus is composed of different subdetectors. Next figure shows a sketch of it, from top to bottom:

- a time of flight system, ToF (S1, S2, S3);
- an anticoincidence system (denoted in the figure as CARD, CAT, CAS);
- a magnetic spectrometer;
- an electromagnetic imaging calorimeter;
- a shower tail catcher scintillator (S4);
- a neutron detector.

The PAMELA experiment (2006-2016)



The AMS-02 Experiment

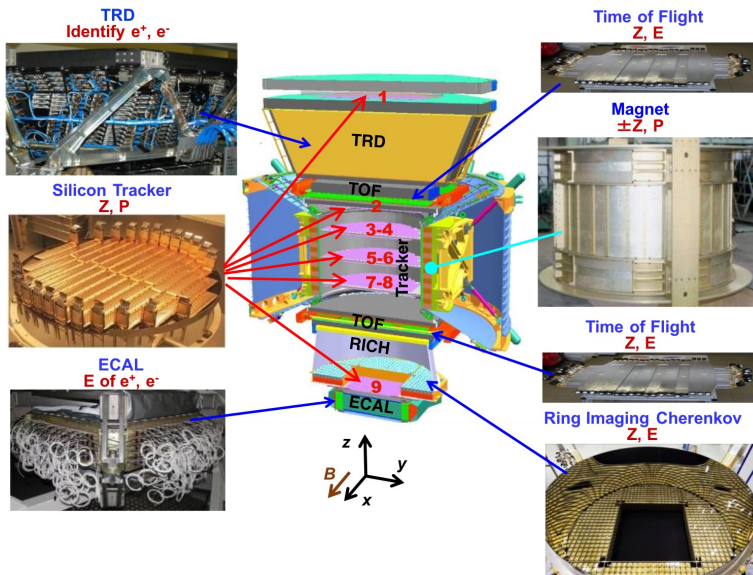
The **Alpha Magnetic Spectrometer AMS-02** is the largest particle physics detector ever carried outside the atmosphere. It was designed to operate as an **external module on the International Space Station (ISS)**. It studies the cosmic ray composition and flux up to tens of TeV.

It was launched on **16th May 2011 on board of the shuttle Endeavour. The mission duration is expected to coincide with the lifetime of the ISS (still alive).**

The AMS-02 prototype was designated as **AMS-01**. It was a simplified version of the detector, which **flew into space aboard the Space Shuttle Discovery in June 1998 for about 10 days**. AMS-01 proved that the detector concept worked in space and provided some important measurements.

AMS-02 utilizes 15 among particle detectors and supporting subsystems in a volume of 64 m^3 ; its weight is 8500 kg and it dissipates 2.5 kW. Its subdetector system is a sort of compendium of devices carried by preceding satellites and balloon experiments. For this reason, we describe it with some details. Next picture will sketch its main sub-detectors.

The AMS-02 Experiment



Calorimetric experiments

PAMELA and AMS-2 are experiment based around a **spectrometer**, thus allowing to detect **matter versus antimatter**.

As we have seen already - in parallel to this - scientists use experiments based only on the **calorimetric technique** for the direct determination of charged cosmic rays. This technique allows to **reach higher energies**.

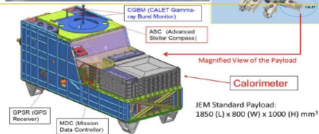
Among many of such experiment, we need to mention **CALET (ISS)**, **DAMPE (satellite)**, **FERMI (satellite)** and **HEPD-01 (satellite)**, still in data-taking like AMS.

Great contributions to Cosmic Ray measurements in recent years have been done also by **ISS-CREAM (ISS)** and **NUCLEON (satellite)** space missions.

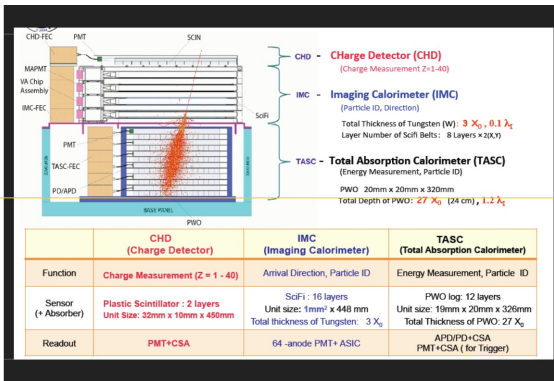
CALorimetric Electron Telescope "CALET"

Launched August 19th, 2015, on ISS. Sensitive to:

- ◇ electrons: from 1 GeV to 20 TeV
- ◇ protons and nuclei (up to Z=40): tens of GeV to hundreds of TeV
- ◇ diffuse gamma emission and GRBs



Continues stable observation since Oct. 13, 2015 and collected ~1.8 billion events so far.



Dark Matter Particle Explorer “DAMPE”

Launched December 17th, 2015. Sensitive to:

- ◇ protons and nuclei: 100 GeV – 100 TeV
- ◇ electrons and gammas: 5 GeV – 10 TeV




Jiuquan Satellite Launch Center
December 17th, 2015

Satellite-borne particle detector, project of the Strategic Pioneer Program on Space Science, promoted by the Chinese Academy of Sciences (CAS).

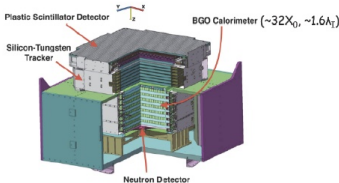
ALTITUDE: 500 km
PERIOD: 95 minutes
ORBIT: Sun-synchronous



- Study of Cosmic Rays composition, origin and propagation
- Search for Dark Matter signatures in lepton and photon spectra
 - High Energy Gamma-Ray Astronomy



DAMPE Instrument



- Charge measurement (dE/dx in PSD, STK and BGO)
- Gamma-ray converting and tracking (STK and BGO)
- Precise energy measurement (BGO Crystals)
- Hadron rejection (BGO and Neutron Detector)

(Chang et al. Astropart.Phys. 95 (2017) 6–24)

Large Area Telescope onboard “Fermi”

Launched June 11th, 2008.

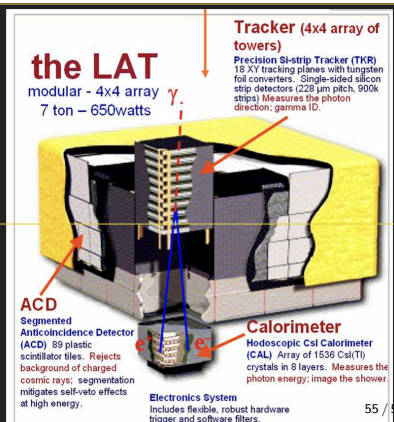
Gamma-ray space detector, but sensitive to:

◇ electrons and positrons: 20 – 200 GeV



The Fermi Gamma-ray Space Telescope circles Earth every 96 minutes in a 26° inclination orbit at an altitude of 535 km.

Fermi carries two scientific instruments, the Large Area Telescope (LAT) and the Gamma-ray Burst Monitor (GBM).



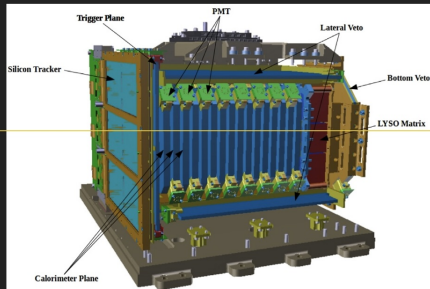
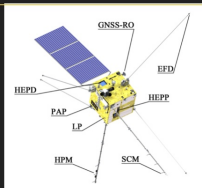
The High Energy Particle Detector on CSES-01

Launched on Feb. 18th, 2018. Sensitive to

- ◇ protons: 30 - 300 MeV
- ◇ electrons: 3 - 100 MeV
- ◇ light nuclei: up to a few hundreds of MeV



The CSES-01 satellite is based on the Chinese CAST2000 platform and moves in a sun-synchronous orbit at 500 km altitude and with an orbital inclination of approximately 98°. It hosts several payloads, among them HEPD-01

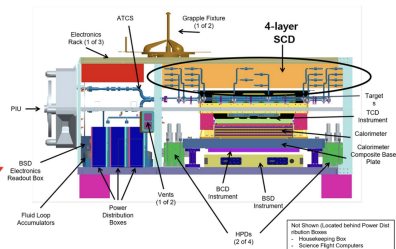
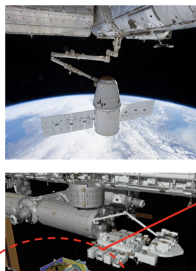


HEPD-01 functional scheme

ISS-CREAM experiment (2017 - 2019)

Launched on Feb. 18th, 2018. Sensitive to:

◇ nuclei ($Z = 1-26$): 1 TeV — 1 PeV.



Direct measurement (TeV – PeV)

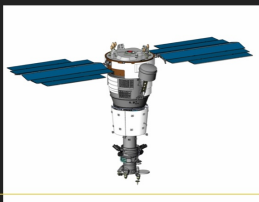
Silicon Charge Detector (SCD) : Charge measurement, tracking
C-Target & Calorimeter (CAL) : Energy measurement, tracking, trigger
Top/Bottom Counting Detector (TCD & BCD) : e/p separation, trigger
Boronated Scintillator Detector (BSD) : e/p separation by neutron detection

- Launch : Aug. 14, 2017
- Data taken period : Aug. 22, 2017 ~ Feb. 12, 2019 (~ 539 days)
- Design to direct measurement of high-energy cosmic rays

NUCLEON experiment (2014-2017)

Launched on Feb. 18th, 2018. Sensitive to:

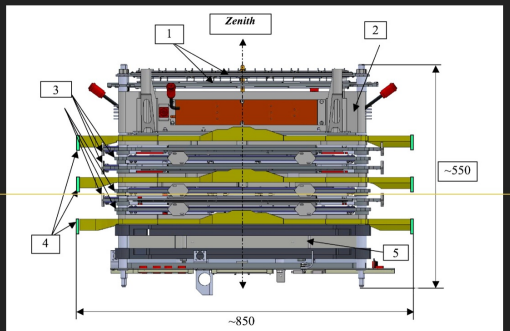
◇ nuclei ($Z = 1-26$): 100 GeV — 1 PeV.



Apparatus mounted aboard the RESURS-P2 satellite.

Sun-synchronous orbit with an inclination of 97° and an altitude of 475 km.

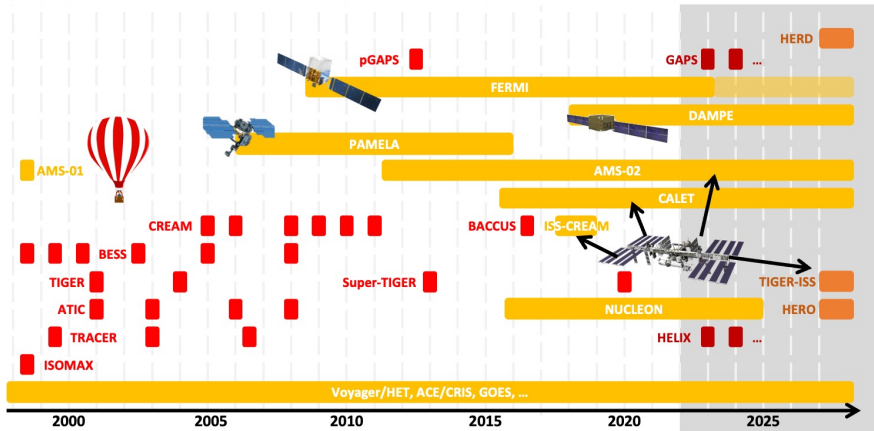
KLEM technique.



A simplified layout diagram of the NUCLEON spectrometer. 1 - two pairs of planes of the charge measurement system (ChMS); 2 - a carbon target; 3 - six planes of the energy measurement system using the KLEM method (KLEM system tracker); 4 - three double-layer planes of the scintillator trigger system (the trigger system); 5 - a small aperture calorimeter (IC).

Timeline of Direct Measurement of CRs from 2000

4



Great legacy from the past (<2000), here we focus on the latest ones. Not all experiments displayed (sorry).
Many different techniques, frequently focusing on some specific CR species or energy range.